SOME EXPERIMENTS ON FREE DROPLET COMBUSTION AT LOW GRAVITY

J.C. Yang, G.S. Jackson, and C.T. Avedisian
Sibley School of Mechanical and Aerospace Engineering
Cornell University, Ithaca, N.Y. 14853

ABSTRACT

A small-scale (7.6m) drop tower was used for studying the combustion of unsupported fuel droplets (about 500μm initial diameter) in a stagnant ambience under low gravity. The experimental procedure consisted of generating a droplet in a near vertical trajectory and then releasing the chamber within which the droplet was introduced, as well as associated instrumentation, into free-fall when the droplet reached the apex of its trajectory.

Some results of the burning of n-heptane, toluene, and heptane/hexadecane mixture droplets are reported. The range of the heptane data is discussed in terms of possibly varying ambient conditions around the droplet during burning due to droplet motion. Microexplosions were not observed for the mixture reported.

1. INTRODUCTION

Experiments on the combustion of unsupported droplets that used gravity as the parameter through which buoyancy effects were minimized have been carried out in drop towers in which the test droplet, its enclosed environment (i.e., the combustion chamber containing the air within which the droplet was burned), and associated instrumentation were simultaneously released into free-fall[1-4]. The test droplets were formed by first holding captive the liquid sample by one or more fibers or needles and then freeing the sample from the fiber(s) by a jerking motion of the fiber(s) along its axis. The droplets produced by this method were large (~1000μm initial diameter) by comparison to droplet sizes that are encountered in most practical combustion situations—typically less than 100μm (e.g., burning sprays). In an effort to study droplets of sizes more characteristic of those likely to be encountered in practical applications, we recently reported on a different technique for generating smaller free droplets—in the range of 400μm to 500μm diameter[5]. While it may be argued that droplets in this size range are still too large to yield results representative of those encountered in practical applications, the present effort is a step in that direction.

This paper summarizes some of our recently obtained experimental results on the combustion of free droplets of n-heptane, toluene, and a mixture of n-heptane and n-hexadecane in a low gravity environment. The experiments were conducted in room temperature air at 0.101 MPa.

2. EXPERIMENTAL METHOD

A schematic diagram of the drop tower facility is illustrated in Figure 1. It consisted of: 1) a vertical shaft; 2) an upper work station with movable floor cover to expose the drop shaft; 3) a drop package which was made of an aluminum and steel support framework and which contained the droplet generator, combustion chamber, spark ignition system, high-speed motion picture camera, and light source; 4) a hoist system; 5) an electromagnet for holding and releasing the drop package, 6) a deceleration tank; and 7) a timing control circuit. Further details may be found in Reference 5.

The idea was to first generate droplets at a rate of 2 drops/s in a steady stream of

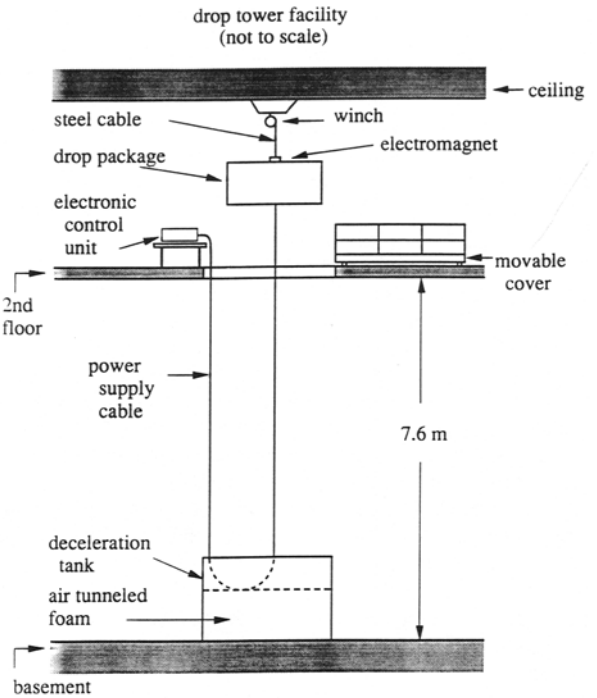

Figure 1

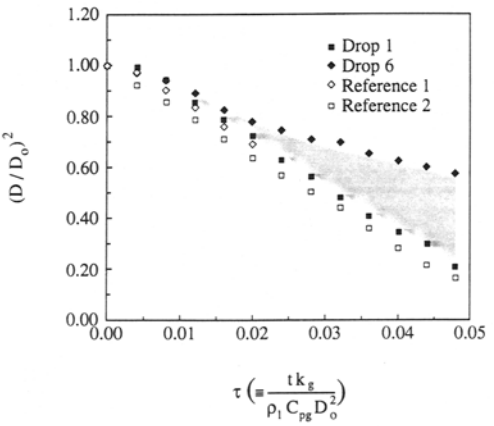

Figure 2

mono-dispersed droplets between 400μm and 500μm diameter; smaller droplets were not studied due to difficulties of optical resolution. The droplet trajectories were almost vertical. The stream was then shut off and the last droplet of this stream was used to perform the experiment. When this last droplet was near the apex of its trajectory, it was ignited by spark discharge across two electrodes positioned around the apex. The drop package was then released into free fall. The droplets studied exhibited a small velocity that was created by inaccuracies in timing the release of the platform with the time of flight of the droplet to its apex, or by the small horizontal velocity component of the droplet due to its non-vertical trajectory. The cumulative effect of these motions yielded Reynolds numbers (*Re* based on droplet diameter) on the order of a maximum of 0.1.

The gravity levels experienced in the moving frame of reference with the present experimental set up were on the order of 10^{-3} that of earth normal gravity. The corresponding Grashof number (based on the initial droplet diameter) was on the order of 10^{-5} (see Appendix). Droplets larger than 1000μm diameter require lower gravity levels to achieve the same dynamic effect. For example, doubling the droplet diameter (from 500μm to 1000μm) would require reducing gravity by about an order of magnitude if all other parameters were held constant. The use of an air drag shield around the drop package to further reduce gravity is an option which has not yet been exploited in the present experimental design.

The primary means of data acquisition was photographic. A 16mm high speed movie camera was operated at 250 frames/s to record the droplet burning history. Direct back lighting was provided by a single tungsten halogen projector lamp. The light intensity used did not permit the flame to be observed for heptane droplets because our initial efforts were directed at obtaining shadow images of the droplets.

Droplet dimensions were obtained directly from the film record by a frame-by-frame analysis. A 16mm film projector was used to vertically project the droplet image onto a horizontal drafting board. The projector lens was positioned approximately 65cm above the board. With this arrangement the operator could focus the image while remaining seated, which facilitated accurate focusing of each frame. Projected droplet images at ignition ranged between 1.5cm and 2 cm. Maximum horizontal and vertical diameter measurements were obtained by marking lines with a pencil with a 0.3mm lead. From these measurements, the equivalent diameter was calculated as the diameter of a sphere with the same volume as the droplet, assuming an ellipsoidal droplet. The greatest source of error in data reduction involved visually identifying the boundary between the droplet and background. In this respect, the present method may be expected to yield comparable accuracy to that obtained from a Vanguard™ analyzer, but is not as rapid as more automated systems[6].

3. RESULTS AND DISCUSSION

3.1 Single Component Hydrocarbons

Results from n-heptane droplets are summarized in Figure 2 in nondimensional form to suppress the effects of initial droplet diameter. The shading indicates the range of six observations, with the evolution of droplet diameter reported for the droplets which burned the fastest and slowest. Figure 3 provides representative shadow photographs from these six heptane droplets (drop 7 was a heptane/hexadecane mixture to be discussed in Section 3.2); for each set the enlargement is uniform, but different enlargements were used for each of the photographic sets. Drops 2 to 6 were captured on the downward side of their trajectories and were thus drifting downward toward the nozzle exit during the period of low gravity; drop 1 was captured near to the apex and drifted laterally (to the right). The maximum Reynolds numbers and initial diameters are listed in Table 1. Only data in the time

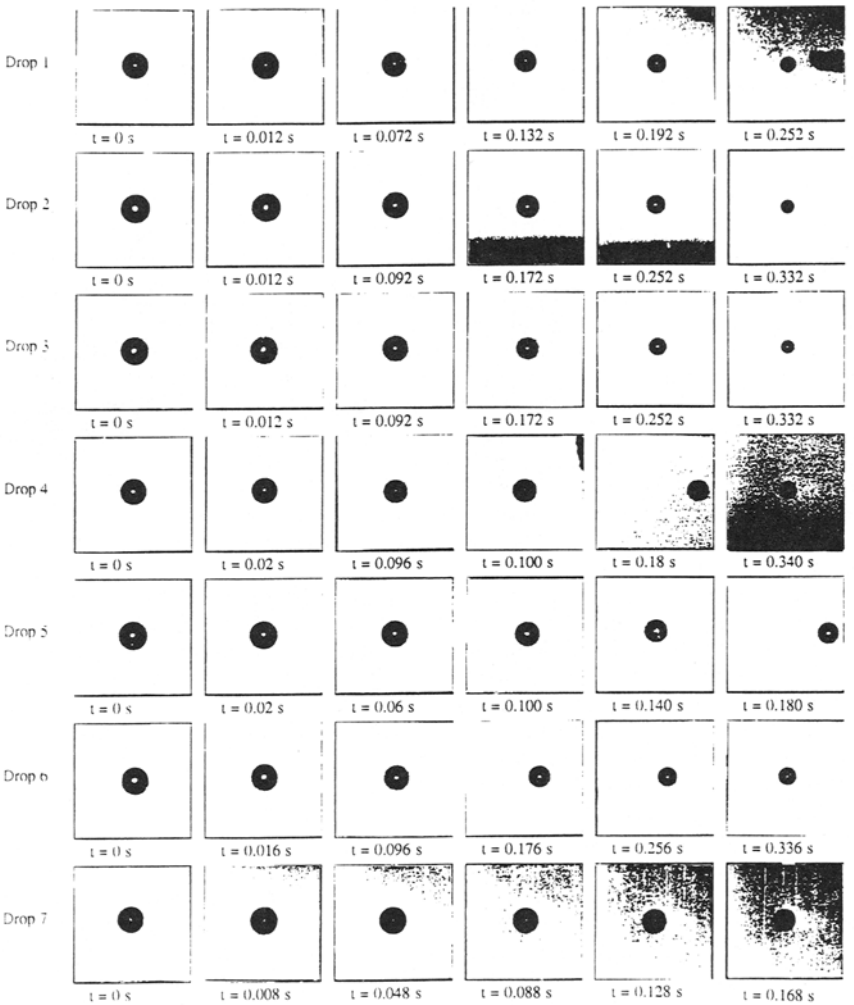

Figure 3

domain from ignition but prior to extinction and/or vaporization-like phenomenon are included in Figure 2.

Table I
Initial Diameter and Maximum Reynolds Numbers for Droplets Reported in Figure 3

Drop Number	Initial Diameter (mm)	Maximum Reynolds Number ($VD\rho/\mu$)
1	0.50	0.058
2	0.45	0.11
3	0.43	0.078
4	0.44	0.082
5	0.43	0.097
6	0.42	0.096
7	0.49	0.058

Two facts to note are that the flame is not visible in the photographs shown in Figure 3, and that for the six heptane droplets studied (the evolution of diameters of which fell in the shaded region bounded by drops 1 and 6 in Figure 2), the burning rates were not constant and exhibited values during burning which ranged between 0.5 mm^2/s and 0.78 mm^2/s. We note that because the burning rate is obtained by essentially differentiating the data, it is very sensitive to uncertainties in the measurements and the range of data selected to define it, particularly if the evolution of droplet diameter squared is not linear throughout the entire period of burning (cf, drop 6 in Figure 2). If the evolution of D^2 is not linear over the period of burning (which may have been due to effects in the present experiment that are conjectured below), the burning rate will be time dependent.

The maximum burning rate among the heptane droplets studied (drop 1) is similar to previously reported unsupported droplet measurements carried out at low gravity[1,2]. Lower values are considered to be attributed to: 1) variations of the convective flow around the droplets during burning; 2) size-dependent effects from different initial droplet diameters; 3) irregularities in the spark's interaction with the droplet and the surrounding gases; 4) soot shell geometry and its effect on the heat transfer rate to the droplet; and/or 5) variations in the gas concentration, most notably the oxygen concentration, during burning.

The low Reynolds numbers (based on droplet diameter) of the droplets studied makes it unlikely that an axial vapor flow around the droplets could significantly influence the burning rate. The maximum Reynolds numbers were well in the Stokes flow regime as shown in Table 1. Based on standard corrections to the droplet burning rate which account for forced convective motion around burning droplets[7], the ranges in Figure 2 could not be due simply to variations in Re from droplet to droplet. In addition, the burning rate is also dependent on the droplet diameter. However, the range of initial diameters shown in Table 1 is not sufficiently large to explain the range[1] shown in Figure 2.

The spark ignition may influence the burning process because of its inherent transience and its uneven heating of the surrounding gas. In the present method, ignition was thought to be achieved by the spark heating gases into which the droplet moved as it was rising to its apex. The spark did not come in direct contact with the droplet. Droplet ignition was manifested by a visible yellow plume near the droplet which disappeared within 40 msec. However, it is not clear that these ignition characteristics play a significant role in the main portion of the burning. Further investigations are being pursued to assess the effect of spark location and energy, and multiple electrode configurations[4], upon the droplet burning process.

The burning rate increases with ambient oxygen concentration[8]. Pre-existing fuel vapors in the vicinity of the droplet at ignition would tend to lower the initial oxygen concentration there below the far-field ambient concentration. Since the experiment required a continuous stream of droplets to achieve a steady trajectory, fuel vapors could have accumulated during the preparatory stage of an experiment from some pre-vaporization of these droplets, both in the parabolic path traversed by the stream and in the recessed region adjacent to the generator nozzle support as the droplets in the continuous stream entered this region. A droplet ignited in this oxygen lean surrounding and drifting about within it would then burn more slowly than in the far ambience.

If fuel vapor accumulation occurred in the parabolic path of the continuous stream, it was evidently below the lean flammability limit because ignition of these vapors was not observed. A fuel rich zone near the nozzle exit caused by vaporization of liquid fuel accumulating there during preparation of an experiment (i.e., during the period in which the relevant timing parameters are being measured for the stream), could be envisioned to have created a concentration gradient of fuel (and oxygen) vapors such that the fuel (oxygen) concentration decreased (increased) from a peak (minimum) near the nozzle exit toward the apex. A droplet drifting downward toward the nozzle would then experience a decreased oxygen concentration and thus burn progressively more slowly. Drops 2 to 6 were captured just on the downward side of their trajectories and were drifting toward the nozzle, though not necessarily in a straight line. The entrance to the nozzle "well" can be seen in the fourth and fifth photograph for drop 2, and the sixth photograph for drop 4 in Figure 3. The slowest burning rate of the six droplets reported with downward trajectories in Figure 3 was drop 6, and these data are plotted in Figure 2. Unfortunately, it has not yet been possible to sample the gas phase around the droplet to quantify its composition. The effect of gas composition on the droplet burning rate bears on the physical property values and the transfer number.

Drop 1 exhibited a lateral movement after ignition which is considered to have brought it into a zone characterized by the standard ambience after being ignited. The evolution of the diameter for this droplet is similar to prior measurements[1,2] as shown in Figure 2.

Due to the intense background illumination and the camera framing rate used (250 frames per second), neither the particularly "bluish" flame around the n-heptane droplets nor the extent of soot around the heptane droplets could be observed so it is an open question as to whether extensive sooting of small heptane droplets such as studied here occurs. However, toluene droplets were also studied with the existing optical set-up, and it was found that toluene droplets sooted extensively. For this liquid the light emitted from the toluene flame and soot around toluene droplets was sufficient to expose the film as shown in Figure 4, in contrast to heptane (Figure 3).

Figure 4a and 4b show two representative photographic images of a toluene droplet taken just after ignition, and well into burning, respectively. Figures 4c and 4d show computer-generated images of the photographs displayed in Figures 4a and 4b. The images enhance the flame and soot boundaries, and clearly reveal the flame shape. Two zones are revealed: an outer luminous region which probably defined the primary reaction zone of the flame, and an inner carbon or soot ring between the droplet surface and the outer region. Initially, a carbon shell penetrated across the outer luminous zone of the droplet (Figure 4c) and then the shell began to break up as it became spherical (Figure 4d) revealing a perhaps fragile shell structure.

It can be conjectured that the soot shell thickness and the location of the droplet within it should effect the droplet burning rate. One thought is that the soot shell can introduce a thermal resistance for heat transfer between the droplet surface and flame thereby reducing the heat transfer rate and the droplet burning rate.

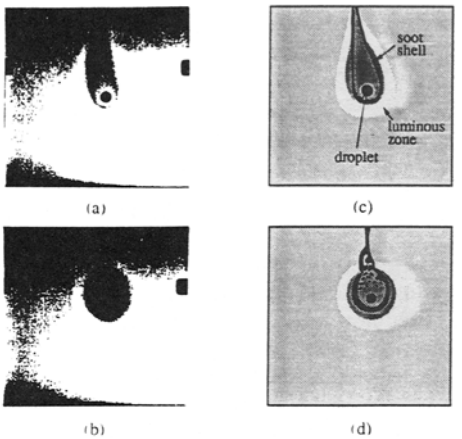

Figure 4

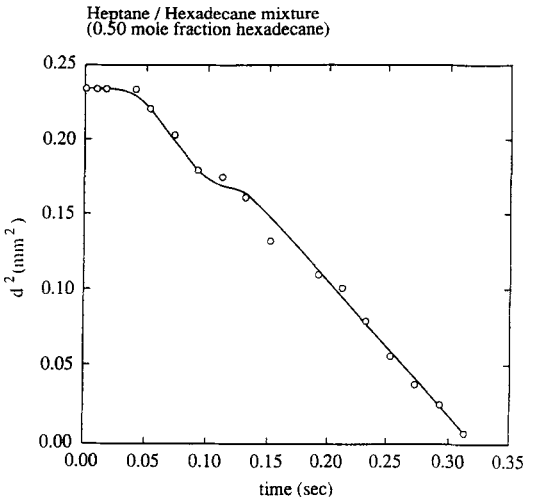

Figure 5

Another perspective is that the hot soot particles can increase the heat transfer rate to the droplet since the soot particles would reside closer to the droplet than the flame. In either event, if the ratio of the soot to the droplet radius is not constant during burning, caused perhaps by varying drifting trajectories of the droplets from run to run and a difference in the relaxation time for the shell to respond to movement changes of the droplet (or vice versa), the burning rate would vary as well from run to run.

Single component unsupported droplets have been observed to explode during their combustion at low gravity. The phenomenon was first identified as "flash extinction" by Knight and Williams[3], and later studied in more detail by Shaw *et al.*[4] using decane droplets about 1 mm initial diameter. The small heptane droplets studied here were not observed to explode (at least the droplet size at which such explosions may have occurred was too small to be optically resolved); no mention of explosions was made in connection with the heptane experiments of Hara and Kumagai[2] which involved a droplet of about 920μm initial diameter. The phenomenon might somehow be sensitively dependent on droplet motion, initial droplet size, method of droplet deployment or ignition, soot shell or flame structure, etc., as these aspects relate to the formation and movement of the soot shell with respect to the droplet.

3.2 Binary mixtures

The mixture components were chosen to yield nearly ideal solutions in order to facilitate physical property predictions which might be required in future model development. The mixture components studied thus far were heptane and hexadecane.

Figure 5 shows the temporal variations of the square of the droplet diameter for one particular 0.5 mole fraction hexadecane in heptane mixture. These data come from drop 7 in Figure 3. Similar trends were also observed for a 0.33 and 0.75 mole fraction hexadecane in heptane mixture. Droplet heating was revealed by an initial period after ignition during which the droplet diameter was approximately constant. Such heating has also been shown to prevail in the combustion of multicomponent droplets at earth normal gravity[9,10].

The solid line in Figure 5 is a curve of best fit, which was drawn to represent a possible trend of droplet diameter squared. The data are not sufficient to conclusively show the typical three-stage burning that has been observed for certain types of miscible mixtures of liquids. One reason could be the resolution of the photographic images, but this is just conjecture. There may be evidence, though, that between 0.1 s and 0.15 s after ignition hexadecane began to dominate the vaporization process. The solid line was drawn to lend support to that possibility. Such a change would indicate a form of preferential vaporization previously observed by others[10].

Microexplosions were not observed for the heptane/hexadecane mixtures (at atmospheric pressure) over the range of compositions studied. Theoretical predictions of this phenomenon are based on the droplet temperature and its superheat limit commensurate with the droplet composition and ambient pressure. If the droplet temperature exceeds the superheat limit of the liquid, microexplosions are possible, though the extent to which the process can shatter the droplet depends on the rate of growth of the initial bubble.

A very simple model considered that the temperature at the edge of the mass diffusive boundary layer within a multicomponent droplet (where the temperature was assumed to vary linearly), commensurate with the liquid phase Lewis number, dictated whether or not the droplet had the potential for microexplosions[11]. If this temperature is compared with the predicted superheat limit for a heptane/hexadecane mixture[12], it is seen to be below the superheat limit for the liquid compositions studied at 0.101MPa. However, if the droplet temperature is taken as spatially

uniform and equal to the boiling point of hexadecane, then the occurrence of homogeneous nucleation within the droplet is more likely. The literature has revealed situations in which an unsupported heptane/hexadecane mixture droplet has[13] and has not[10] undergone microexplosion at earth normal gravity. Gravity alone will not effect the superheat limit of a liquid. However, the method of droplet deployment, soot formation around the droplet, etc., could possibly influence the liquid composition within the droplet and thereby the superheat limit, the droplet temperature, and thus the propensity for microexplosions.

ACKNOWLEDGEMENT

This study was supported by the National Science Foundation through Grant No. CBT-8451075 and the New York State Center for Hazardous Waste Management. This support is gratefully acknowledged.

REFERENCES

1. S. Okajima & S. Kumagai, 1975. *15th Symp. (Int.) Comb.*, pp. 401-407.
2. H. Hara & S. Kumagai, 1988. Poster No. P257 *22nd Symp. (Int.) Comb.*
3. B. Knight & F. A. Williams, 1980. *Comb. Flame* **38**, 111-119.
4. B. D. Shaw, F. L. Dryer, F. W. Williams, & J. B. Haggard, 1987. Paper No. IAF-87-403, International Astronautical Congress, Brighton, England, 10-17 October.
5. C. T. Avedisian, J. C. Yang, & C. H. Wang, 1988. *Proc. Roy. Soc. London*, *A***420**, 183-200.
6. M. Y. Choi, F. L. Dryer & J. B. Haggard, 1989. This volume and chapter.
7. C. K. Law & F. A. Williams, 1972. *Comb. Flame* **19**, 393-405.
8. M. Goldsmith, 1956. *Jet Propulsion* **26**, 172-178.
9. B. J. Wood, H. Wise & S. H. Inami, 1960. *Comb. Flame* **4**, 235-242.
10. C. H. Wang, X. Q. Liu,& C. K. Law, 1984. *Comb. Flame* **56**, 175-197.
11. T. Niioka & J. Sato, 1986. *21st Symp. (Int.) Comb.*, pp. 625-631.
12. C. T. Avedisian & J. R. Sullivan, 1984. *Chem. Eng. Sci.*, **39**, 1033-1041.
13. J. C. Lasheras, A. C. Fernandez-Pello, & F. L. Dryer, 1980. *Comb. Sci. Tech.* **22**, 195-209.
14. Task Group on Fundamental Physics and Chemistry, National Research Council, 1988. **Space Science in the Twenty-First Century.** Chapter 5, National Academy Press, Washington, D.C. .

APPENDIX

The intent of the experimental design was to create a low buoyancy environment. However, gravity alone does not dictate the extent to which buoyancy induced flows will be minimized in our experiment. That is, there is no single acceptable gravity level below which buoyancy induced flows can be neglected[14]. Similarly, there is no single minimum acceptable droplet velocity for the effective free stream flow around the droplet to have a negligible effect on the radial flow field. For a nonzero gravitational level and a nonzero droplet velocity there will be an axial vapor flow around the droplet.

The criterion for neglecting buoyancy induced flows around the droplet is that the Grashof number be small, that is

$$Gr_D \ll 1 \tag{1}$$

where

$$Gr_D = g\beta(T_f - T_\infty)D^3\rho^2/\mu^2 \tag{2}$$

Similarly, effective forced convective flow around the drop may be neglected when

$$Re_D \ll 1 \tag{3}$$

where

$$Re_D = U_\infty Dr/\mu \tag{4}$$

There are several length scales upon which calculation of *Gr* and *Re* can be based,

for example the droplet diameter D or the flame diameter D_f. D is apparently a convenient length scale for correlating droplet burning data as evidenced by the relatively large number of correlations for the burning rate which have used this length scale in the definition of the Grashof and Reynolds number for burning droplets[7].

Equations 1 and 2 show that lowering gravity is one of *several* ways to minimize buoyancy in a droplet experiment. To further illustrate, consider an ideal gas where $\beta \sim 1/T_\infty$, $\rho \sim P/(RT_\infty)$ and with $\mu \sim T_\infty^{1/2}$. The criterion for neglecting buoyancy induced flows and droplet motion becomes

$$C_1(T_f - T_\infty)\, P^2\, D^3 g/T_\infty^4 \ll 1 \qquad \text{[to neglect buoyancy]} \qquad (5)$$

and

$$C_2 U_\infty\, D\, P/T_\infty^{3/2} \ll 1 \qquad \text{[to neglect droplet motion]} \qquad (6)$$

where C_1 and C_2 are constants with the appropriate units. Equation 5 shows that there are four ways by which buoyancy effects can be minimized (all of which have been exploited in the literature): 1) lower g; 2) carry out the experiment at low pressure, 3) reduce the droplet radius; or 4) increase the ambient temperature. Equation 6 shows that not only can U_∞ be reduced, but the droplet radius or pressure can be reduced as well to achieve the same dynamic effect.

The restrictions on droplet velocity are less severe, though perhaps more difficult to satisfy experimentally, than on gravitational level because $Gr_{Rs} \sim D^3 g$ while $Re_{Rs} \sim DU_\infty$. For example, if the initial droplet diameter is doubled from 500μm initial diameter which characterizes our experimental method to, say, 1000μm which is typical of all previously performed low gravity droplet combustion experiments, then the gravity must be reduced by nearly an order of magnitude ($\{0.5/1\}^3$) to yield an equivalent dynamic effect. If droplets in the 2mm to 5mm diameter range are to be studied, then gravity must be reduced yet further from the present 10^{-3} g level to about 10^{-5} g and 10^{-6} g, respectively.

For the conditions of the present experiment, we follow the prescription of Law and Williams[7] to arrive at the following property estimates: $\rho \sim 2.68 \times 10^{-4}$ g-cm^{-3} (air), $\mu \sim 4.96 \times 10^{-4}$ g-cm^{-1}-s^{-1}(air), $T_f \sim 2300$°K, $T_\infty \sim 300$°K, $\beta \sim 7.69 \times 10^{-4}$°K^{-1}, and $g \sim 0.98$cm/s^2 (for the present experiment). Since $D \sim 0.05$cm, Equation 1 shows that $Gr_D \leq 5.5 \times 10^{-5}$. If the characteristic length scale is chosen as the flame radius, and we further assume that $D_f/D \sim 10$, then $Gr_{Df} \sim 5.5 \times 10^{-2}$.

FIGURE CAPTIONS

Figure 1 Drop tower facility.

Figure 2 Comparison of the variation of non-dimensional droplet diameter squared $(D/D_o)^2$ with non-dimensional time t of the present heptane data with those reported in References 1 and 2: $k_g = 0.1141 \times 10^{-2}$ W/cm K; $\rho_l = 0.6139$ g/cm^3; $C_{pg} = 4.283$ J/g K. Data from References 1 and 2 were interpolated.

Figure 3 Photographic sequences from six heptane runs (Drop 1 to Drop 6), and a 0.5 mole fraction hexadecane in heptane mixture (Drop 7).

Figure 4 A burning toluene droplet. Figures 4a and 4b show direct back-lighted photographs taken 0.056 s and 0.136 s respectively after ignition (total burning time for this droplet was 0.364 s). Figures 4c and 4d are computer-generated images of the photographs shown in Figures 4a and 4b.

Figure 5 Variation of diameter squared with time for a 0.50 mole fraction hexadecane in heptane mixture droplet.